PERGAMON

Journal of Structural Geology 21 (1999) 743–750

JOURNAL OF STRUCTURAL GEOLOGY

Flow controlled inverted metamorphism in shear zones

Bernhard Grasemann[a,*], Jean-Claude Vannay[b,1]

[a]*Institut für Geologie, Universität Wien, A-1090 Wien, Austria*
[b]*Institut de Minéralogie et Pétrographie, Université de Lausanne, CH-1015 Lausanne, Switzerland*

Received 18 May 1998; accepted 16 March 1999

Abstract

Numerous processes and models have been developed in order to explain inverted metamorphism in shear zones. This article demonstrates, by means of continuum mechanics, that the orientation of a sample profile across a shear zone before and after deformation can be used to quantify the conditions under which inverted metamorphism is likely to have developed. A thrusting shear zone deforming under ideal simple shear will develop an inverted metamorphic zonation if the angle between the thrust and isotherms is greater than 5–10°, even at only moderate strains. If the flow is general shear, this angle is considerably larger (i.e. $>60°$ for a kinematic vorticity number of $W_k = 0.5$). Additionally, the stretch of the sample profile across the shear zone, which is not influenced by the flow type, bears important implications for the interpretation of petrological, geochronological and structural data. Although this kinematic model is clearly an end-member model, neglecting dissipative processes, it can easily account for the structural and petrological data of the inverted metamorphism observed throughout the Higher Himalayan Crystalline wedge in the Sutlej Valley (India). © 1999 Elsevier Science Ltd. All rights reserved.

1. Introduction

Most models developed to explain inverted metamorphism appeal to heat conduction, heat advection, heat production or combined thermo-mechanical processes to account for the observations (e.g. Le Fort, 1975; Graham and England, 1976; Jaupart and Provost, 1985; Molnar and England, 1990; Grasemann, 1993; Jamieson et al., 1996). However, because inverted metamorphic zones are generally observed in rock sequences intensely deformed by ductile flow, another group of models invoking folding and/or shearing can explain inverted metamorphism by displacement (e.g. Frank et al., 1973; Searle and Rex, 1989; Grujic et al., 1996; Hubbard, 1996). Here, the second group of models, particularly the simple shear model of Hubbard (1996), is examined in more detail. Although the approach is very similar to Hubbard (1996), the use of *material lines* is clarified. Furthermore, the model of Hubbard (1996) is expanded to include general non-coaxial flow, using continuum mechanics. The paper focuses explicitly on the first order effects of deformation flow in shear zones and completely neglects dissipative processes. Thus, by implication, only rocks which are cooling during deformation are considered.

2. Definitions

In the following text, the process of thrusting a hanging wall over a footwall in a shear zone of finite width is called *deformation*. The state before and after displacement is called *undeformed* and *deformed*, respectively. *Normalized offset* (γ_n) is defined as the maximum shear zone-parallel component of finite displacement divided by the initial thickness of the shear zone. Therefore γ_n has no physical dimension and is equal to the shear strain (γ) in cases of ideal simple shear.

Material lines are imaginary lines connecting an

* Corresponding author.
E-mail address: Bernhard.Grasemann@univie.ac.at (B. Grasemann)
[1] *E-mail address:* Jean-Claude.Vannay@imp.unil.ch

0191-8141/99/$ - see front matter © 1999 Elsevier Science Ltd. All rights reserved.
PII: S0191-8141(99)00071-1

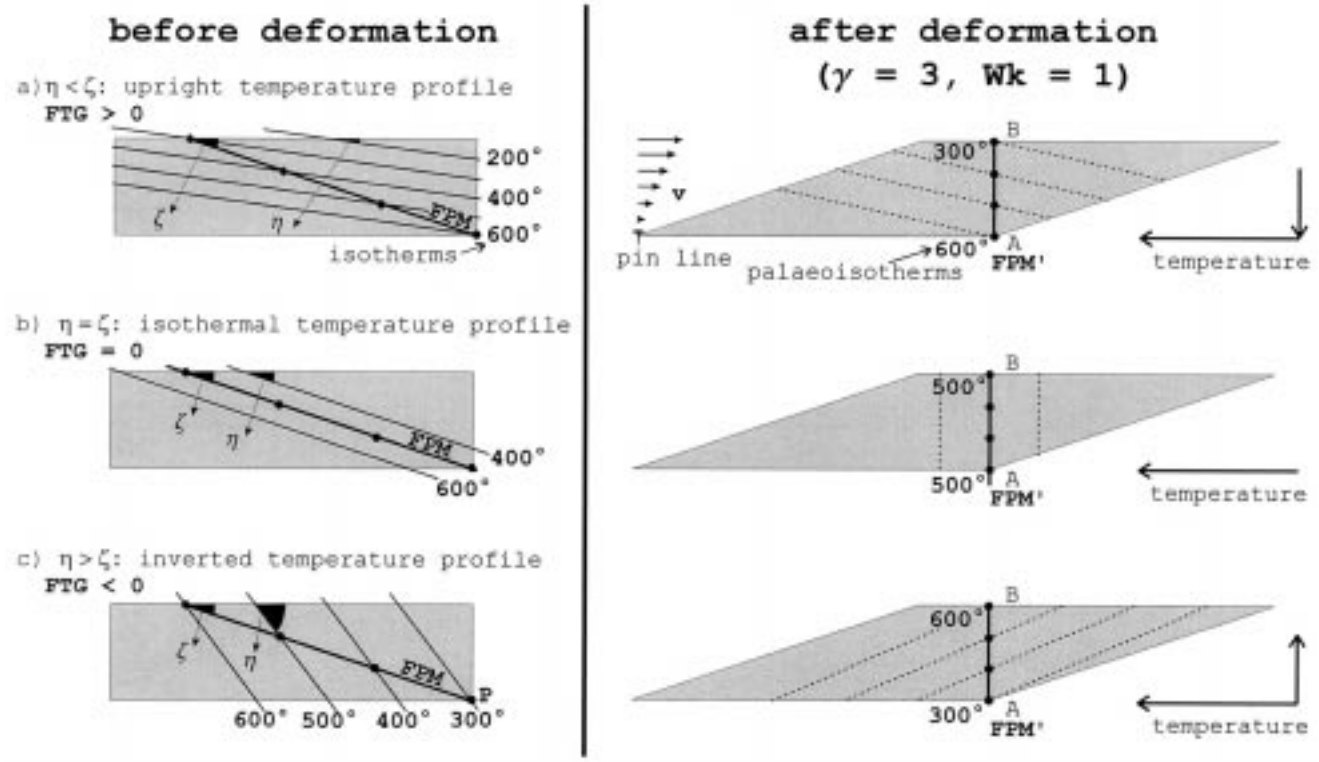

Fig. 1. The left column shows the shear zone of a thrust, the FPM and the isotherms in the undeformed state. The right column shows the shear zone, the FPM′ and the palaeoisotherms in the deformed state ($\gamma = 3$, $W_k = 1$). (a) If the isotherms are flatter dipping than the FPM with respect to the shear zone ($\zeta > \eta$), an upright temperature profile (FTG $>$ 0) will develop. (b) The isotherms are parallel to the FPM ($\zeta = \eta$) and consequently FTG = 0. (c) If the isotherms are steeper dipping than the FPM with respect to the shear zone ($\zeta < \eta$), an inverted temperature profile (FTG $<$ 0) will develop.

array of points or physical features at a single instant in time. Since these lines behave passively, their position in physical space is only influenced by the flow during a shear zone's deformation history. Therefore, isotherms are *not* material lines because, due to conduction and/or heat production, these lines do not behave passively during deformation. Material lines after deformation that were parallel to the isotherms before deformation are here called *palaeoisotherms*. These are different from the classical definition of *isograds*, which represent lines of constant metamorphic grade and are commonly defined by index minerals. Since the index minerals along an isograd probably did not form at the same time, isograds are *not* material lines. However, if rocks only cool after peak metamorphism, and if the first appearance of an index mineral is mainly temperature controlled, isograds can be used as an approximation to palaeoisotherms, so long as deformation post-dates metamorphism (as in the case of the proposed model). More accurate measurement of palaeoisotherms can be made by oxygen isotope studies (e.g. Bottinga and Javoy, 1973).

Much confusion has been generated by the various definitions of inverted metamorphism. Whereas some authors based their definition on an inverted sequence of metamorphic isograds (e.g. Frank et al., 1973; Searle and Rex, 1989; England and Molnar, 1993; Hubbard, 1996), other studies related inverted metamorphism to palaeotemperatures increasing structurally up-section (e.g. Swapp and Hollister, 1991; Ruppel and Hodges, 1994; Macfarlane, 1995; Jamieson et al., 1996), even though in some instances, the sampled profile was subhorizontal and no evidence was given to show that the palaeotemperature profile was inverted (i.e. palaeohot on top of palaeocold!).

Where rocks sampled across a shear zone reveal an inverted palaeotemperature profile, we only know that an imaginary line connecting these sample localities from the bottom to the top of the shear zone experienced increasing peak temperatures. Therefore, the orientation of this material line before deformation is of central interest. In the following, this material line, which represents a hypothetical profile across a shear zone and which is oriented perpendicular to the shear zone *after* deformation, is called FPM′ (finite perpendicular material line). The same line in the undeformed state is called FPM (Fig. 1).

The angle between the shear zone boundary and the

FPM ζ is related to the normalized offset by (angles in physical space are measured clockwise throughout this work):

$$\tan \zeta = \gamma_n^{-1} \quad (1)$$

The angle between the shear zone boundary and the initial pre-deformation isotherms is η. Only η-angles between 0 and 90° are considered. If $\eta > 90°$, the initial isotherms are inverted and consequently any flow-type (including pure shear) causing thrusting will result in an inverted palaeotemperature profile.

3. Upright, isothermal and inverted palaeotemperature profiles

In shear zones that undergo homogeneous deformation (i.e. flow parameters are constant through time) and where the orientation of the flow eigenvectors is fixed in the external reference frame (steady-state flow), the magnitude and orientation of the velocity vectors are strongly dependent on their position within the shear zone (Ramberg, 1975). A shear zone deforming under simple shear with a pin-line at its lower boundary shows increasing magnitudes of velocity and displacement vectors from the bottom to the top (Fig. 1a). Consequently, any passive marker line inclined against the shear direction will rotate in the shear direction due to the higher velocities at the top and the lower velocities at the bottom of the shear zone. During rotation, the material line will shorten at decreasing rates until it is aligned perpendicular to the shear zone. At this position the incremental longitudinal strain is zero (Ramsay and Huber, 1983).

Assuming that during deformation the rocks within the shear zone are not increasing in temperature, the initial orientation of the FPM with respect to the isotherms can be used to quantify the model configurations where an inverted metamorphic profile can develop. Note that the metamorphic pressure recorded by rocks along the FPM′ is—besides the flow type of deformation—a function of the initial orientation and depth of the shear zone. However, neither the orientation of the shear zone in the external frame of the crust nor the external spin of the shear zone during deformation is considered in this study. The temperature gradient along a profile can be quantified using a *finite temperature gradient* (FTG) which is simply defined by:

$$\mathrm{FTG} = \frac{T_A - T_B}{\overline{AB}} \quad (2)$$

Where $\overline{AB}$ is the distance between A and B (Fig. 1). T_A and T_B are the temperatures at points A and B, respectively, which are the intersections of the FPM′ with the lower and upper shear zone boundaries, respectively. Depending on the sign of the FTG, the following situations can be distinguished (Fig. 1):

(i) FTG > 0, upright palaeotemperature profile, $\eta < \zeta$ (Fig. 1a): If the dip of the isotherms with respect to the shear zone boundary before shearing is shallower than the dip of the FPM, the resulting FPM′ will always record an upright palaeotemperature profile.
(ii) FTG = 0, isothermal palaeotemperature profile, $\eta = \zeta$ (Fig. 1b): If the isotherms are parallel to the FPM, the palaeoisotherms after deformation will be parallel to the FPM′ and consequently all samples collected along a FPM′ will record the same temperature.
(iii) FTG < 0, inverted palaeotemperature profile, $\eta > \zeta$ (Fig. 1c): If the dip of the isotherms with respect to the shear zone boundary before shearing is steeper than the dip of the FPM, the resulting FPM′ will always record an inverted palaeotemperature profile.

Comparing Fig. 1(a–c), the following important points can be observed:

(i) If the FTG ≥ 0, the distance between rock samples collected along palaeoisotherms after deformation is always shortened. If the FTG < 0, the distance between rock samples collected along palaeoisotherms after deformation can be shortened, equal or stretched relative to their original distance depending on the shear strain. For large γ, this distance will always be markedly stretched.
(ii) If the FTG ≥ 0, the distance between the palaeoisotherms after deformation is greater than the distance between the isotherms before deformation. If the FTG < 0, the distance between the palaeoisotherms after deformation can be greater, equal to or shorter than the distance between the isotherms before deformation. For large γ this distance will be always markedly shortened.
(iii) Rocks sampled normal to the shear zone boundary can record increasing, decreasing or uniform temperatures. Rocks sampled parallel to shear zone boundary and parallel to the stretching lineation always record increasing temperatures towards the root zone.
(iv) If the Eulerian position gradient tensor, which relates the position of any points in the deformed state to coordinates in the undeformed state, can be determined, the undeformed state of the shear zone can be restored. In this case, η can be calculated if the palaeoisotherms can be detected in the field.
(v) If the Eulerian position gradient tensor is known, the pre-deformational depth and dip of the

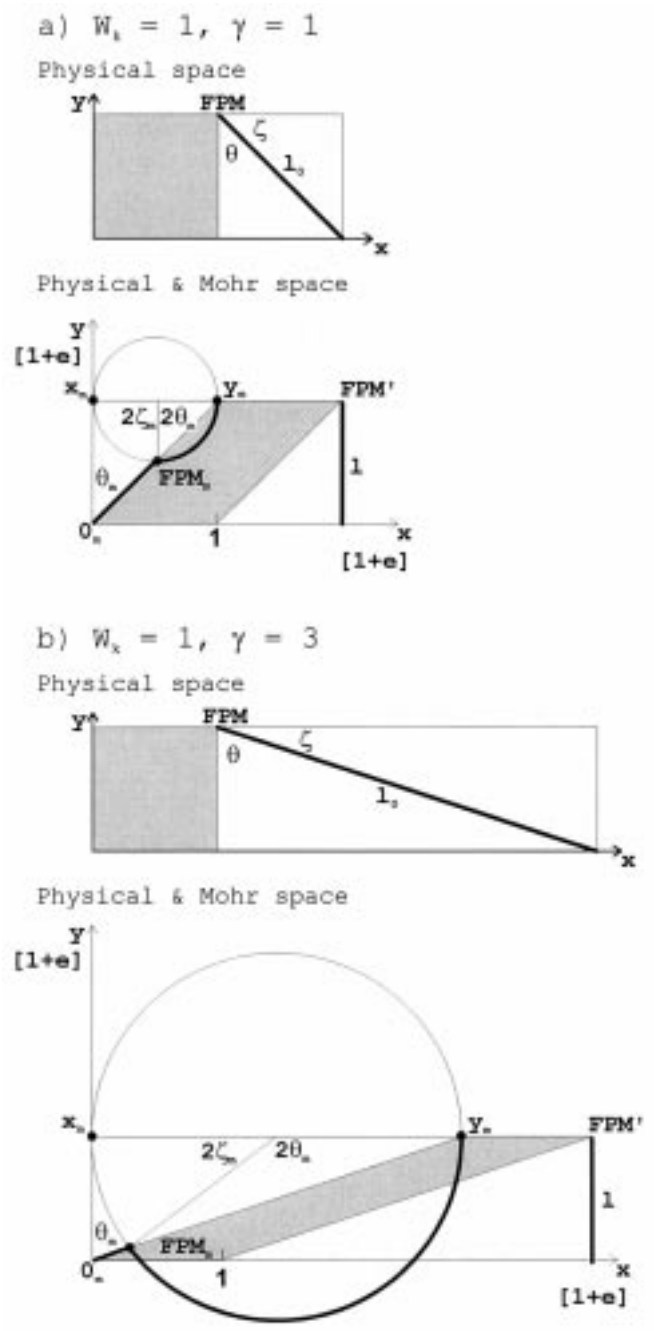

Fig. 2. Physical space and Mohr space (variables in the Mohr space are indicated with subscript m) of unit square deforming by simple shear: (a) $\gamma = 1$ and (b) $\gamma = 3$. With increasing γ, the stretch of the FPM (O_m–FDM_m) decreases significantly. The sector of possible θ where the deformation would result in an inverted temperature profile increases.

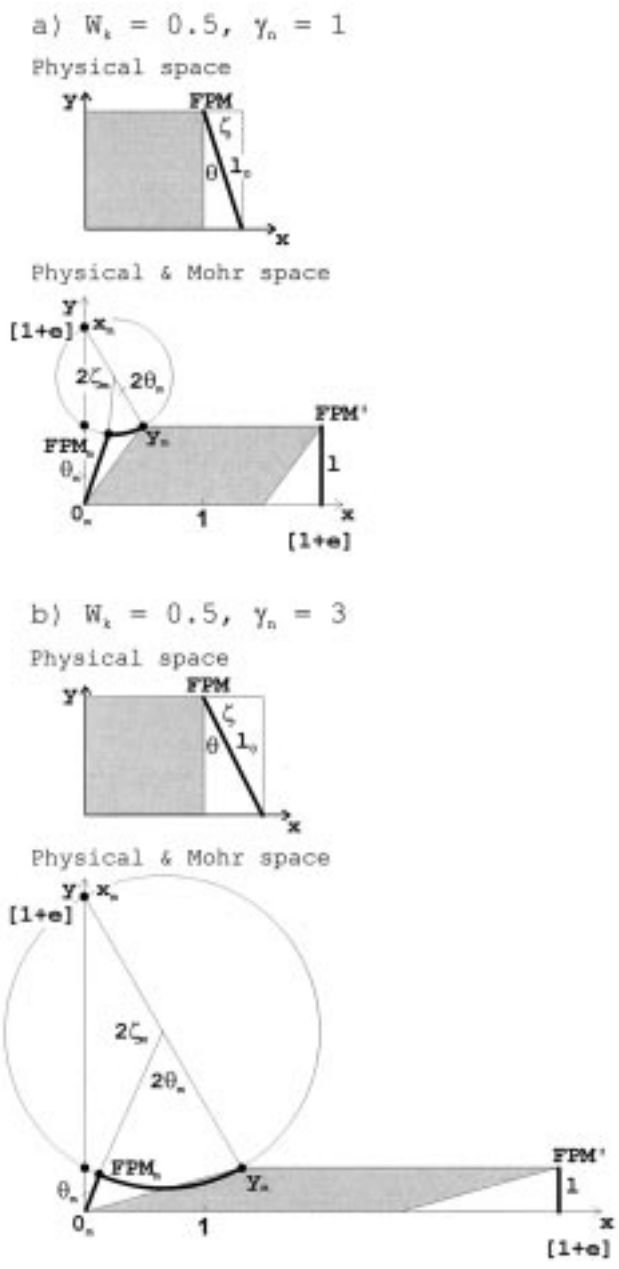

Fig. 3. Physical space and Mohr space of a unit square deforming with general shear ($W_k = 0.5$): (a) $\gamma_n = 1$ and (b) $\gamma_n = 3$. Although the stretch of the FPM is very similar to the simple shear deformation, the sector of θ-angles where the deformation would result in an inverted temperature profile is considerably smaller.

shear zone can be calculated from the pre-deformational lithostatic peak pressures and the pressure gradient recorded by the rocks collected along the FPM′. The external spin of the shear zone can be thus determined by comparing the shear zone orientation before and after deformation.

(vi) The cooling age pattern recorded along the FPM′ reflects the time at which the rocks along this material line crossed the isotherm corresponding to the blocking temperature of the chosen geochronological system during shearing. Neglecting the deformation-controlled perturbation of the isotherms, which is only likely in very special tectonic situations (e.g. during extrusion of orogenic wedges,

where conductive heat loss to the hanging wall and footwall of the wedge is balanced by advection of heat within the wedge; Hodges et al., 1993), the following age distribution trend along the FPM′ can be inferred (note that the model presented is not intended as a forward modeling tool for thermochronological data but outlines the effects of a shear zone being exhumed through a fixed thermal frame).

If the FTG ≥ 0 the shear zone will always record older cooling ages at the top and younger ages at the bottom. Where the FTG < 0, three different cooling trends can develop, depending on the blocking temperature of the applied thermochronological method: (a) If the blocking temperature is higher than the isotherm that passes through the lower intersection point of the FPM and the shear zone boundary (point P in Fig. 1c), then the lower part of the FPM rotates through the blocking temperature first and so cooling ages at the top of the shear zone will be younger and ages at the bottom will be older. (b) If the blocking temperature is equal to the isotherm that passes through P (i.e. 300°C isotherm in Fig. 1c), then all rocks will record the same cooling age. (c) If the blocking temperature is lower than the isotherm that passes through P, then cooling ages at the top of the shear zone will be older and ages at the bottom will be younger.

It is important to note that many other effects—mainly dissipative processes—can obscure the presented cooling pattern during thrusting. Therefore this discussion just highlights the effects of deformation, which are neglected in other models focusing on thermal effects. Besides the processes of heat advection, heat production and heat conduction, which are likely to occur during natural thrust tectonics, this simple modeling of the effects of deformation shows that thermochronological methods have a limited use in interpreting inverted metamorphism.

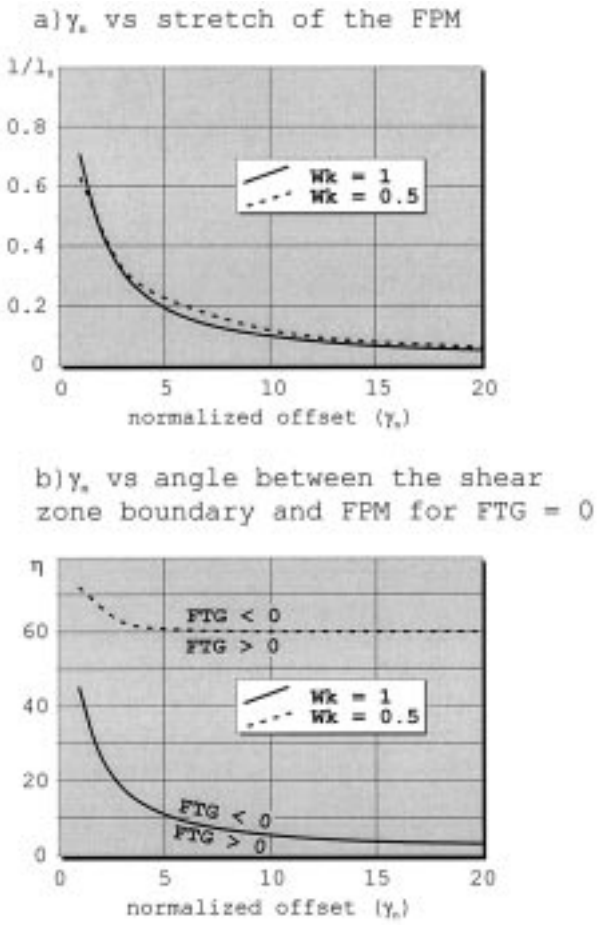

Fig. 4. Plots for (a) stretch of the FPM and (b) orientations of isotherms with respect to the shear zone (η), which would result in an isothermal temperature profile, for $W_k = 1$ and 0.5 vs γ_n. The stretch is very similar for both flow types, but the curves for η are markedly different: For simple shear ($\gamma_n > 10$), initial angles greater than 5° between the isotherms and the shear zone boundary are sufficient to result in a FTG < 0. General shear ($W_k = 0.5$) will result in high ($\eta \sim 60°$), even if the γ_n is large.

4. Inverted temperature gradient: simple vs general shear flow

The influence of increasing γ_n is illustrated by means of Mohr circle constructions of the second kind for the Lagrangian position gradient tensor $\mathbf{F}_{ij}$ (Figs. 2 and 3). Finite deformation is conveniently described by $\mathbf{F}_{ij}$ relating the position of any material point in the deformed state to coordinates in the undeformed state. $\mathbf{F}_{ij}$ contains information on finite strain, volume change and rigid body rotation. De Paor and Means (1984) have shown that for any tensor with components a, b, c and d, the points (b, d) and (c, a) in Mohr space specify the diameter of a Mohr circle of the second kind. This Mohr space coincides with physical space. In the case of $\mathbf{F}_{ij}$, Means (1982) has shown that the polar co-ordinates of points on the Mohr circle are equal to the stretch and the angle of rotation of material lines after a given finite strain. Additionally, the counterclockwise double angle measured between points along the circle is equal to twice the clockwise angle between these lines in real space in the undeformed state. With this we can conveniently describe stretch and rotation of the FPM and investigate the effects of increasing strain and various flow types.

Fig. 2(a) shows the physical space of a unit square with the FPM in the undeformed state and the Mohr circle with the deformed unit square and FPM′ for ideal simple shear ($W_k = 1$, $\gamma = 1$). The Cartesian x- and y-coordinate axes are parallel and normal to the shear zone boundary before deformation. ζ is the

angle between the shear zone boundary and FPM. θ is the angle between the FPM and the normal to the shear zone boundary. The FPM and FPM′ have a length of l_0 and l, respectively. In the Mohr circle diagram (material lines and angles plotting in the Mohr space are indicated with subscript m), points plotting on the y_m-axis represent material lines which are not rotating. In the case of ideal simple shear, only lines parallel to x do not rotate. In the undeformed state x is perpendicular to y and consequently x_m and y_m specify the diameter of the Mohr circle. The angle between FPM_m and y_m is $2\theta_m$. The thick line O_m–FPM_m gives the stretch (l/l_0) of the FPM′ after deformation. The rotation of FPM′ is given by the angle θ_m between FPM_m–O_m and the y_m-axis. The thick arc between FPM_m and y_m indicates the initial orientation of isotherms where the applied deformation would result in an FTG < 0 (i.e. inverted metamorphism).

Comparing Fig. 2(a) and (b) it can be seen that at higher γ, the stretch of the FPM′ (thick line O_m–FPM_m) decreases dramatically whereas θ increases. In other words, increasing γ implies that even small initial angles between the shear zone and the isotherms will result in inverted palaeotemperature profiles.

Fig. 3 is similar to Fig. 2 but the flow within the shear zone is non-dilatant general shear ($W_k = 0.5$). Contrary to simple shear deformation, a second non-rotating direction (i.e. eigenvector) develops. Additionally, there is a significant stretching component parallel to the shear zone boundary. Although the stretch of the FPM′ is very similar in the simple shear and general shear model, θ is considerably smaller in Fig. 3. This is obvious in the Mohr space where the arc length FPM_m–y_m is considerably shorter in the general shear than in the simple shear models. Thus, the angle between the shear zone boundary and the isotherms deforming with general shear has to be significantly larger than in ideal simple shear zones in order to result in an inverted palaeotemperature profile.

5. Discussion

In order to demonstrate the effect of increasing γ_n, Fig. 4 illustrates the stretch and the angle between the shear zone boundary (η) and the isotherms. In this diagram the FPM′ records an isothermal palaeotemperature profile, calculated for a flow with $W_k = 0.5$ and 1, respectively.

Fig. 4(a) shows that the stretch of the FPM′ calculated by both the simple and the general shear model has *very similar values*. However, for both flow types, the decrease in the stretch of the FPM′ with increasing γ_n is dramatic: $\gamma_n > 5$ will result in a stretch of less than 0.2. Therefore, the distances between samples collected along the FPM′ will be dramatically shorter than the original distance between the samples before onset of deformation. This observation bears important but easily overlooked implications for the interpretation of petrological and geochronological data from rocks sampled across thick zones of high strain (Hubbard, 1996).

Fig. 4(b) shows that there is a *dramatic difference* in η between the simple and general shear model, where the FPM′ records an isothermal palaeotemperature profile. Note that isotherms initially oriented parallel to the FPM plot along the curves, whereas the areas above and below the curves would characterize angles of isotherms resulting in an FTG < 0 and FTG > 0, respectively. For simple shear and $\gamma_n > \sim 5$, initial angles between the shear zone boundary and the isotherms of less than 10° can result in an FTG < 0. General shear ($W_k = 0.5$) requires $\eta \sim 60°$, even if the γ_n is very large. These observations have important consequences for shear zones revealing an inverted palaeotemperature gradient and a significant pure shear component: the initial angle between the shear zone boundary and the isotherms must have been large.

In the Sutlej Valley (NW India), the High Himalayan Crystalline (HHC) is a 10 km thick, highly deformed, high-grade metamorphic sequence bounded by the Main Central Thrust (MCT) at the base and by a normal fault at the top. *P–T* path results suggest that the rocks of the HHC have only cooled during decompression, which has been accommodated by thrusting and synchronous normal faulting (Vannay and Grasemann, 1998). Thermobarometry and oxygen isotope thermometry results indicate that the peak temperatures increase upward throughout this wedge, with palaeoisotherms parallel to the mylonitic foliation and in an inverted position. However, peak temperatures were reached at an almost constant depth, implying that the isotherms in the HHC were dipping toward the foreland and that they were thus significantly oblique with respect to the direction of thrusting along the MCT (Vannay and Grasemann, 1998).

Several models have been proposed to explain the Himalayan inverted metamorphism and it is interesting to discuss the relevance of the main models with reference to the Sutlej section. An inversion of isograds due to syn- to post-metamorphic, large-scale recumbent folding or tectonic imbrications (e.g. Searle and Rex, 1989) is not consistent with the constant pressure field gradient throughout the Sutlej HHC, as well as with the absence of tectonic discontinuities between the mineral zones. The 'hot iron' model (Le Fort, 1975) invokes a transient inversion of the geotherm at the level of the MCT, as a result of heat conduction between the hanging wall and footwall of the thrust. This model predicts a retrograde metamorphic evol-

ution in the hanging wall of the MCT and peak temperatures increasing upwards to reach a maximum at some structural level within the HHC. Such features do not appear consistent with the absence of significant retrograde metamorphism in the hanging wall of the MCT. The shear heating model (e.g. Molnar and England, 1990), considering the effect of heat production by friction at the level of the MCT, predicts a maximum temperature at the level of the thrust. In contrast, the lowest temperatures of the Sutlej section are observed at the level of the MCT.

In the Sutlej Valley, material lines in the HHC represented by the palaeoisotherms have been significantly rotated during flow to inverted positions, whereas the material line connecting the sampled rocks did not rotate as indicated by the equal lithostatic pressures. These observations require a second (shortening) eigenvector, which indicates a general shear flow (Ramberg, 1975). Inasmuch as quantitative kinematic field observations demonstrate that the HHC extrusion was associated with intense general shear deformation throughout the unit, a ductile shearing of the palaeoisotherms towards the direction of thrusting could explain the inverted metamorphic zonation in the Sutlej section (Grasemann et al., 1999).

It should be emphasized that the results of this study isolate the influence of deformation on the final distribution of exhumed rocks in a shear zone of a thrust, which experienced only cooling during deformation, and thus represent only a first order approximation if the model assumptions are justified. For a geodynamic model of natural thrusts, many other time-dependent processes such as heat conduction, heat advection, heat production, fluid flow, mechanical and rheological aspects, have to be considered.

6. Conclusions

1. Simple shear-dominated flows within shear zones can easily result in an inverted palaeotemperature profile, even at moderate finite strain.
2. Flows within shear zones having a significant pure shear component need a high angle between the shear zones and the isotherms in order to result in an inverted palaeotemperature profile. Examples of such high angles could be the result of a higher geothermal gradient in the hanging wall than in the footwall or a steep dip of the shear zone.
3. The distance between rocks sampled across a shear zone is usually dramatically shortened even at moderate finite strain. This consideration bears important consequences for the interpretation of analytical data derived from these samples (e.g. pressure, temperature, cooling age, exhumation rate).
4. Inverted palaeotemperature profiles can record cooling ages which have all the same age or which become continuously older or younger towards the top of the shear zone. Consequently, syn-deformational cooling ages from shear zones need cautious interpretation.
5. Although this kinematic model is clearly an end-member model, neglecting dissipative processes, it can easily account for the structural and petrological data of the inverted metamorphism observed throughout the HHC wedge in the Sutlej Valley.

Acknowledgements

We thank Hugh Rice, Neil Mancktelow, Kurt Stüwe, Erich Draganits and Gerhard Wiesmayr for fruitful discussions and for reviewing the manuscript. The authors acknowledge support from the Austrian 'Fonds zur Förderung der wissenschaftlichen Forschung' (FWF grant P-11765-GEO) and the Swiss National Science Foundation (FNRS grants 20-45063.95). Very careful reviews and important suggestions of the associate editor R.J. Norris and R.A. Jamieson and comments by an anonymous reviewer were much appreciated.

References

Bottinga, Y., Javoy, M., 1973. Comments on oxygen isotope geothermometry. Earth and Planetary Science Letters 20, 250–265.

De Paor, D.G., Means, W.D., 1984. Mohr circles of the First and Second Kind and their use to represent tensor operations. Journal of Structural Geology 6, 693–701.

England, P., Molnar, P., 1993. The interpretation of inverted metamorphic isograds using simple physical calculations. Tectonics 12, 145–157.

Frank, W., Hoinkes, G., Miller, Ch., Purtscheller, F., Richter, W., Thöni, M., 1973. Relations between metamorphism and orogeny in a typical section of the Indian Himalayas. Tschermaks mineralogische und petrographische Mitteilungen 20, 303–332.

Graham, C.M., England, P.C., 1976. Thermal regimes and regional metamorphism in the vicinity of overthrust faults: an example of shear heating and inverted metamorphic zonation from southern California. Earth and Planetary Science Letters 31, 142–154.

Grasemann, B., 1993. Numerical modelling of the thermal history of the NW Himalayas, Kullu Valley, India. In: Treloar, P.J., Searle, M.P. (Eds.), Himalayan Tectonics, 74. Geological Society Special Publication, pp. 475–484.

Grasemann, B., Fritz, H., Vannay, J.-C., 1999. Quantitative kinematic flow analysis from the Main Central Thrust Zone (NW-Himalaya, India): implications for a decelerating strain path and the extrusion of orogenic wedges. Journal of Structural Geology. 21, 837–853.

Grujic, D., Casey, M., Davidson, C., Hollister, L.S., Kündig, R., Pavlis, T., Schmid, S., 1996. Ductile extrusiom of the Higher Himalayan Crystalline in Bhutan: evidence from the quartz microfabrics. Tectonophysics 260, 21–43.

Hodges, K.V., Burchfiel, B.C., Royden, L.H., Chen, Z., Liu, Y., 1993. The metamorphic signature of contemporaneous extension and shortening in the central Himalayan orogen: data from Nyalam transect, southern Tibet. Journal of Metamorphic Geology 11, 721–737.

Hubbard, M., 1996. Ductile shear as a cause of inverted metamorphism: example from the Nepal Himalaya. Journal of Geology 104, 493–499.

Jamieson, R.A., Beaumont, C., Hamilton, J., Fullsack, P., 1996. Tectonic assembly of inverted metamorphic sequences. Geology 24, 839–842.

Jaupart, C., Provost, A., 1985. Heat focussing, granite genesis and inverted metamorphic gradients in continental collision zones. Earth and Planetary Science Letters 73, 385–397.

Le Fort, P., 1975. Himalayas: The collided range. Present knowledge of the continental arc. American Journal of Science 275, 1–44.

Macfarlane, A.M., 1995. An evaluation of the inverted metamorphic gradient at Langtang National Park, Central Nepal Himalaya. Journal of Metamorphic Geology 13, 595–612.

Means, W.D., 1982. An unfamiliar Mohr circle construction for finite strain. Tectonophysics 89, 1–6.

Molnar, P., England, P.C., 1990. Temperatures, heat flux, and frictional stress near major thrust faults. Journal of Geophysical Research 95, 4833–4856.

Ramberg, H., 1975. Particle paths, displacement and progressive strain applicable to rocks. Tectonophysics 28, 1–37.

Ramsay, J.G., Huber, M.I., 1983. In: The Techniques of Modern Structural Geology, Volume 1: Strain Analysis. Academic Press, London.

Ruppel, C., Hodges, K.V., 1994. Pressure–temperature–time paths from two-dimensional thermal models: prograde, retrograde, and inverted metamorphism. Tectonics 13, 174.

Searle, M.P., Rex, A.J., 1989. Thermal model for the Zanskar Himalaya. Journal of Metamorphic Geology 7, 127–134.

Swapp, S.M., Hollister, L.S., 1991. Inverted metamorphism within the Tibetan Slab of Bhutan: evidence for a tectonically transported heat-source. Canadian Mineralogist 29, 1019–1041.

Vannay, J.-C., Grasemann, B., 1998. Himalayan inverted metamorphism in the High Himalaya of Kinnaur (NW India): petrography versus thermobarometry. Schweizer mineralogische und petrographische mitteillungen 78, 107–132.